

On one-step replica symmetry breaking in the Edwards-Anderson spin glass model

Gino Del Ferraro,¹ Chuang Wang,^{2,3} Hai-Jun Zhou,² and Erik Aurell^{1,4,5}

¹*AlbaNova University Centre, KTH-Royal Institute of Technology*

Dept of Computational Biology, SE-106 91 Stockholm, Sweden

²*State Key Laboratory of Theoretical Physics, Institute of Theoretical Physics,*

Chinese Academy of Sciences, Beijing 100190, China

³*School of Engineering and Applied Sciences, Harvard University,*

33 Oxford Street, Cambridge MA 02138 USA

⁴*ACCESS Linnaeus Centre and Center for Quantum Materials,*

KTH-Royal Institute of Technology, SE-100 44 Stockholm, Sweden

⁵*Depts of Applied Physics and Computer Science,*

Aalto University, FIN-00076 Aalto, Finland

(Dated: May 31, 2022)

We consider a one-step replica symmetry breaking description of the Edwards-Anderson spin glass model in 2D. The ingredients of this description are a Kikuchi approximation to the free energy and a second-level statistical model built on the extremal points of the Kikuchi approximation, which are also fixed points of a Generalized Belief Propagation (GBP) scheme. We show that a generalized free energy can be constructed where these extremal points are exponentially weighted by their Kikuchi free energy and a Parisi parameter y , and that the Kikuchi approximation of this generalized free energy leads to second-level, one-step replica symmetry breaking, GBP equations. We then show that contrary to the analogous case of Bethe approximations in locally tree-like graphs this second-level GBP does not have a class of simpler solutions analogous to Survey Propagation. We attribute this discrepancy to the presence of short loops in a region graph description of the Edwards-Anderson model, and argue that it should be a fairly general phenomenon for redundant region graphs.

I. INTRODUCTION

Low-temperature phases of systems with random interactions can be thought of as optimizing under a large set of highly interdependent and conflicting constraints. If a local optimum has been found it will typically be difficult to improve upon without adjusting many variables over a large domain, which is inherently difficult, for any optimization procedure. A physical process obeying detailed balance will furthermore care not directly about how different are two configurations but rather about how high are the energy barriers between them; for low enough temperature transition

times should follow an Arrhenius law, $\tau_{transit} \sim \tau_{micro} e^{-\beta E_B}$, where τ_{micro} is a (microscopic) attempt time, E_B is a barrier height and $\beta = \frac{1}{k_B T}$ is the inverse temperature. If barrier heights increase with system size N different such low-lying states will be essentially disconnected for very long times (exponential in N), and the equilibrium Gibbs measure separates into a (weighted) sum over such states.

Let the above-mentioned (metastable) states be labeled by k and each characterized, over some long time, by an average energy E_k and a probability distribution P_k with entropy S_k . They can then be considered as having (metastable) free energy densities $f_k = \frac{1}{N} (E_k - TS_k)$ and from these one can construct a second-order statistical mechanics built on a second-order partition function

$$\Xi(y) = \sum_k e^{-\beta y N f_k} \quad (1)$$

which is known as a one-step replica symmetry breaking (1RSB) scheme [1, 2]. The Parisi parameter y in (1) plays the role of an inverse temperature and it is conjugate to a free energy-like quantity (referred to as a generalized free energy) which can be defined as $G(y) = -\frac{1}{\beta y} \ln \Xi$. In the large- N limit the sum in (1) can be expected to be dominated by different subsets of states for different y , and knowing the corresponding maximizing distributions gives, in analogy with standard statistical mechanics, information on the system in the thermodynamic limit. This program has been carried out with great success for dilute systems where the constraints are locally organized in tree-like structures. For such a networks, in the thermodynamic limit, the Bethe approximation is exact when loops are of order of the logarithm of the system size and, at the replica symmetric (RS) level and for single graph instances, it can be computed using the iterative scheme known as Belief Propagation (BP) [3, 4]. Improvements in the performance of this latter algorithm can be obtained by applying the procedure described above to locally-tree like networks which corresponds to break the replicas symmetry in the distributions of the fields (messages). So far this approach has been applied to the first-step of replica symmetry breaking and results are known as 1RSB belief-propagation equations [1, 5], i.e. BP equations for the probability distributions of messages. It has been shown that, among all the possible solutions that these equations admit, there exist a class of them made by probability distributions of one-single message. The resulting theory obtained within this class of solutions is known as Survey Propagation (SP) [5–7] and has been applied in several area from information sciences [1, 8] to neuroscience and other fields [9]. While there are several routes to the SP theory, we will here only be concerned with one where the three crucial ingredients are (i) an efficient computation of f_k using the Bethe approximation, (ii) an approximation of (1) by a Bethe approximation on the second order, and (iii) a reduction of this

approximation to SP, which can also be efficiently computed [1].

Systems in finite dimension are however not arranged in tree-like structures. The above sketched approach is therefore, for a physical system, only valid as a mean-field theory and it is typically also presented as such. There exists a considerable literature as to whether these approaches apply to finite-dimensional systems *cf.* [10–13] – which we will not enter except to point out that the question of barriers, and their heights, is one of geometry and hence strongly dependent on dimensionality. Indeed, even for infinite-dimensional systems much less is known about the distribution of barrier heights than about the distributions of free energy minima, and (1) may therefore, as pertaining to dynamically separate states, even in idealized cases be somewhat of an ansatz.

The Kikuchi (or cluster) expansion was introduced to improve upon the mean-field estimates of thermodynamic quantities [14–16]. Algorithmically it can be turned into Generalized Belief Propagation (GBP) [17–19] which, though considerably more complicated than BP, can be used to estimate marginal probabilities on graphs with short loops and has applications to inference in lattice systems appearing in image processing problems [4]. The question then arises if the local minima of Kikuchi free energy, computed as fixed points of GBP, can be turned into a second-order 1RSB statistical mechanics as in (1), and if that can be efficiently computed in analogy to SP. If that would be the case we could arrive at better systematic approximations to thermodynamics of finite-dimensional random systems, and, perhaps conceptually more important, give a different kind of argument in favor of the spin glass approach in finite-dimensional system. This general issue has been investigated in the recent literature already [20–22], though not by using the same approach that we present here.

In this paper we attempt to address the problem by directly writing a second-order partition function analogous to (1) for the Edwards-Anderson spin glass model in two dimensions, but using instead of Bethe approximation a Kikuchi expansion based on regions containing one, two or four spins (“vertices”, “rods” and “plaquettes”). This leads to a quite complex 1RSB statistical model on second level, where the variables are GBP terms (“GBP messages”) obeying hard-core constraints (“GBP fixed point equations”) and weighted by terms $e^{-\beta y N f_k}$ where the f_k are the Kikuchi free energies computed from the fixed points of GBP. We show how to perform a Kikuchi expansion for this 1RSB second-level model using regions isomorphic to the regions on the RS first level model, and hence also interpretable as (second-level) “vertices”, “rods” and “plaquettes”. In contrast to first level the amount of variables in each second-level region is however large, as will be described in some detail below. We also point out, as far as we know for the first time, that a Kikuchi expansions can be performed in many ways for such a second-level model; our choice is only

one of the simplest. We are thus able to carry through the second step in the approach described above arriving at a definite – though complicated – set of equations which can be interpreted as 1RSB GBP equations which, to the best of our knowledge, have never been derived before. We then show that, in contrast to the path from BP to second-order (1RSB) BP to SP, these equations do not have the same kind of special solutions which can be effectively computed. As we will argue we believe this to be a general result which can be traced back to short loops which the second-level GBP inherits from the first-level GBP. Although we hence essentially demonstrate a negative result, we believe it of interest in highlighting difficulties in systematically treating finite-dimensional systems by spin glass theory methods. In a companion paper we will present another approach to a SP-like theory built on GBP, and which we believe may be more practical [23].

The paper is structured as follows. In Section II we recall the Edwards-Anderson model and outline its main properties as established by numerical methods. In Section III we describe a Kikuchi approximation for this model based on regions “vertices”, “rods” and “plaquettes”, leading to a Generalized Belief Propagation scheme. This presentation follows earlier contributions by two of us [24–26] to which we refer for parts of details. In Section IV we introduce and discuss a second-level GBP scheme and we present, we believe for the first time, the 1RSB GBP equations at the plaquette region-graph level of the Kikuchi approximation. In Section V we show that this scheme does not simplify similarly to the SP case. Although established for one choice of second-level GBP (one second-level region graph) we argue that it should be generally valid for every redundant region graph. In Section VI we sum up and discuss our results.

II. THE EDWARDS-ANDERSON MODEL

The 2D Edwards-Anderson (EA) model [27] is defined on a finite dimensional square lattice by the Hamiltonian $H = -\sum_{(ij)} J_{ij}\sigma_i\sigma_j - \sum_i h_i\sigma_i$, where the first sum is over neighboring spin variables, h_i is a local external field and the J_{ij} are quenched random variables. Using a factor graph representation with N variable nodes ($i = 1, 2, \dots, N$) representing the spins and M factor nodes ($a = 1, 2, \dots, M$) representing the interactions between the spins, the Hamiltonian can alternatively be written as:

$$H(\underline{\sigma}) = \sum_a^M E_a(\underline{\sigma}_{\partial a}) + \sum_i^N E_i(\sigma_i) \quad (2)$$

where $\underline{\sigma} \equiv (\sigma_1, \sigma_2, \dots, \sigma_N)$ denotes a generic spin configuration, and by $\underline{\sigma}_{\partial a}$ we mean $\{\sigma_i | i \in \partial a\}$, the set of variables which are involved in interaction a . In the case of a two dimensional lattice

this is simply $\underline{\sigma}_{\partial a} = \{\sigma_i, \sigma_j\}$, but the more general notation will be convenient later. In the same representation the partition function can be written as:

$$Z(\beta) \equiv \sum_{\underline{\sigma}} e^{-\beta H(\underline{\sigma})} = \sum_{\underline{\sigma}} \prod_{i=1}^N \psi_i(\sigma_i) \prod_{a=1}^M \psi_a(\underline{\sigma}_{\partial a}) \quad (3)$$

where

$$\psi_i(\sigma_i) \equiv e^{\beta h_i \sigma_i}, \quad \psi_a(\underline{\sigma}_{\partial a}) \equiv e^{\beta J_{ij}^{(a)} \sigma_i \sigma_j} \quad (4)$$

are called “potential functions” in the BP terminology. The equilibrium free energy is related to the partition function as:

$$F(\beta) \equiv -\frac{1}{\beta} \ln Z(\beta) \quad (5)$$

The EA model has been extensively studied in the literature with the spin coupling constants J_{ij} following the $\pm J$ bimodal distribution or the continuous Gaussian distribution with zero mean and variance J^2 . If all the external magnetic fields $h_i = 0$, this model is in the spin glass phase when the inverse temperature β exceeds certain critical value β_c . The value of β_c is finite for systems in $D \geq 3$ dimensions, while $\beta_c = \infty$ for $D = 2$, namely the spin glass transition occurs at zero temperature for two-dimensional systems [28–32].

III. REGION GRAPH REPRESENTATION AND GENERALIZED BELIEF PROPAGATION EQUATIONS

In this section we introduce a region graph description of the 2-dimensional lattice and use the Cluster Variation Method (CVM) as presented by Kikuchi [14–16] to compute an approximation to the free energy and derive generalized belief propagation equations as presented in [19, 25, 26]. A region-graph description of a lattice model defines a set R of regions that include some chosen basic clusters of nodes, their intersections, the intersection of their intersections, and so on. The basic idea underlying the CVM is to approximate the free energy as a sum of the free energies of these basic clusters of nodes, minus the free energy of over-counted cluster intersections, minus the free energy of the over-counted intersections of intersections, and so on [18]. Then according to this approach the full probability distribution over all the sites can be expressed in terms of the marginal probability distributions $P_\alpha(\underline{\sigma}_\alpha)$ for each region α

$$P_K(\underline{\sigma}) = \prod_{\alpha} (P_\alpha(\underline{\sigma}_\alpha))^{c_\alpha}. \quad (6)$$

In the expression above the region graph coefficients c_α are counting number assigned to each region to ensure that each term only contributes once [26] and constructed recursively by:

$$c_\gamma = 1 - \sum_{\{\alpha: \alpha > \gamma\}} c_\alpha, \quad (7)$$

where with $\alpha > \gamma$ we indicate that α is an ancestor of γ , i.e. the regions γ is contained in the region α . From (6) we can compute a CVM approximation to the entropy as $S_K(\beta) = -\beta^{-1} \sum_{\underline{\sigma}} P_K(\underline{\sigma}) \log P_K(\underline{\sigma})$ which gives the Kikuchi free energy functional of the $P_\alpha(\underline{\sigma}_\alpha)$'s as

$$F_K = \sum_\alpha c_\alpha \sum_{\underline{\sigma}_\alpha} P_\alpha(\underline{\sigma}_\alpha) \left[U_\alpha(\underline{\sigma}_\alpha) + \beta^{-1} \log P_\alpha(\underline{\sigma}_\alpha) \right] \quad (8)$$

where $U_\alpha(\underline{\sigma}_\alpha)$ is the energy term of the region α , for instance $U_\alpha(\underline{\sigma}_\alpha) = \sum_{i \in \alpha} h_i \sigma_i + \sum_{a \in \alpha} J_{ij}^{(a)} \sigma_i \sigma_j$ in the EA model, whereas $\underline{\sigma}_\alpha \equiv \{\sigma_i | i \in \alpha\}$ denotes a microscopic configuration of the same region. A Kikuchi approximation of the free energy at the R -level then fixes a set R of clusters, made of maximal clusters and all their subclusters, and truncates the expansion of the free energy (8) retaining only terms corresponding to clusters in R . The CVM then aims to the minimization of the above free energy (8) under the constraints that the marginals P_α come from the same full probability distributions. The saddle point equations derived from this minimization are the so called Generalized Belief Propagation equations. A detailed derivation of them, following this standard approach, is provided in Appendix B.

An alternative formulation of the Kikuchi approximation and a derivation of GBP equations can be obtained formulating a region-graph description in terms of factor graphs and messages, i.e. normalized probability distributions, between neighbouring regions. In what comes next we follow such a formulation as described in [26] in order to obtain consistency relations among regions which will be useful in the derivation of the 1RSB Generalized Belief Propagation equations (see Sec. IV). Within this description, generally a region μ can be a parent of another region ν if the set ν is contained in the set μ , and when this is the case we indicate the relation as $\mu \rightarrow \nu$. Hereafter we consider the squares or “plaquettes” to be the larger cluster R and therefore we deal with three types of clusters or regions: plaquettes, rods and vertices, although the description presented next is very general and not restricted to such a maximal clusters. Each square contains four vertices and four interactions and is a parent of four rod regions; each rod region contains two vertices and one interaction and is a parent of two vertices; while each vertex region contains only one vertex and has no children. In Fig. 1, left panel, the parent-to-child relations $\mu \rightarrow \nu$ are represented by black arrows for the regions highlighted in green, namely plaquette, rods and vertices. As mentioned, we

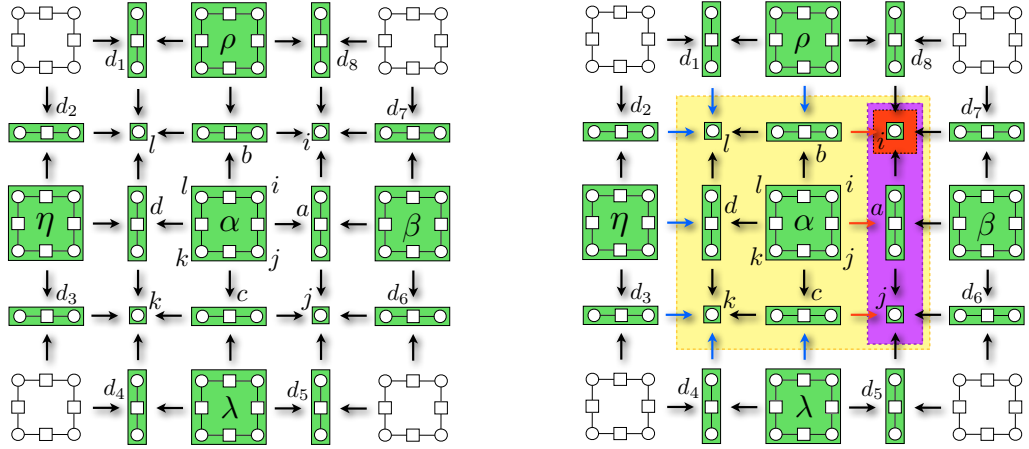


FIG. 1: Left panel: Region graph representation of a 2D EA model in terms of plaquettes, rods and vertices. Black arrows represent parent-to-child relations and are associated with messages from parents to child ($m_{\mu \rightarrow \nu}$ in the main text). Right panel: The squared yellow region represents the union of the border (B_α) and interior (I_α) of the α plaquette. The messages inside it belong to I_α whereas the messages that cross the border belong to B_α . The purple rod region represents the same object for the rod a . Blue and red arrows represent the messages involved in the GBP equation from plaquette α to rod a , namely eq. (22) in the main text.

recursively define an ancestor of a region to be a parent or the parent of an ancestor: a vertex thus has four parents (four rods) and four other ancestors (four plaquettes). Similarly we recursively define a descendant of a region to be a child or the child of a descendant. A plaquette thus has four children (four rods) and four other descendants (four vertices). A region graph R , within this description, is then a collection of all the regions and the specified parent-to-child relations (i.e., arrows) between these regions.

Following [25, 26] the partition function (3) can then be written as

$$Z(\beta) = \sum_{\underline{\sigma}} \prod_{\alpha \in R} \left[\prod_{i \in \alpha} \psi_i(\sigma_i) \prod_{a \in \alpha} \psi_a(\underline{\sigma}_{\partial a}) \right]^{c_\alpha}. \quad (9)$$

where α in principle ranges over all the possible regions. A Kikuchi approximation of this partition function then corresponds to take into account only some chosen set of maximal clusters R in (9), their intersections, the intersection of their intersections, and so on. The Kikuchi approximation of the above partition function then reads as

$$Z_K(\beta) = \prod_{\alpha \in R} \left[\sum_{\underline{\sigma}_\alpha} \prod_{i \in \alpha} \psi_i(\sigma_i) \prod_{a \in \alpha} \psi_a(\underline{\sigma}_{\partial a}) \right]^{c_\alpha} \quad (10)$$

where α ranges over all regions up to a maximal cluster R , for instance restricted to plaquettes, rods and vertices. As already noted in [26] it is possible to introduce sets of messages $m_{\mu \rightarrow \nu}(\underline{\sigma}_\nu)$, i.e.

normalized probability distributions, between parent-child regions in R , with the only constraint that $\sum_{\sigma_\mu} m_{\mu \rightarrow \nu}(\underline{\sigma}_\nu) = 1$. Indeed observing that for each direct edge $\mu \rightarrow \nu$ the following relation holds

$$\sum_{\{\alpha : \mu \in B_\alpha, \nu \in I_\alpha\}} c_\alpha = \sum_{\alpha \geq \nu} c_\alpha - \sum_{\alpha \geq \mu} c_\alpha = 1 - 1 = 0, \quad (11)$$

the Kikuchi partition function (10) can be rewritten as:

$$Z_K(\beta) = \prod_{\alpha \in R} \left[\sum_{\underline{\sigma}_\alpha} \prod_{i \in \alpha} \psi_i(\sigma_i) \prod_{a \in \alpha} \psi_a(\underline{\sigma}_{\partial a}) \prod_{\{\mu \rightarrow \nu : \mu \in B_\alpha, \nu \in I_\alpha\}} m_{\mu \rightarrow \nu}(\underline{\sigma}_\nu) \right]^{c_\alpha}. \quad (12)$$

In (11) and (12) we have for each region α defined $I_\alpha \equiv \{\gamma : \gamma \leq \alpha\}$ to be the set formed by the region α and all its descendants, and B_α , the “boundary” of α , *i.e.* to be the set of regions not belonging to I_α but parental to at least one region in I_α [26] (see Fig 1, right panel). Observe that because of (11) each message appears in (12) net zero times. As a consequence, the Kikuchi approximation to the free energy, in terms of messages $m_{\mu \rightarrow \nu}(\underline{\sigma}_\nu)$, reads as:

$$F_K(\beta) = -\beta^{-1} \sum_{\alpha \in R} c_\alpha \log \left[\sum_{\underline{\sigma}_\alpha} \prod_{i \in \alpha} \psi_i(\sigma_i) \prod_{a \in \alpha} \psi_a(\underline{\sigma}_{\partial a}) \prod_{\{\mu \rightarrow \nu : \mu \in B_\alpha, \nu \in I_\alpha\}} m_{\mu \rightarrow \nu}(\underline{\sigma}_\nu) \right]. \quad (13)$$

Analogously to the standard derivation of the CVM, we then require this free energy to be stationary respect to a chosen set of probability functions $\{m_{\mu \rightarrow \nu}\}$, namely:

$$\frac{\delta F_K}{\delta m_{\mu \rightarrow \nu}} = 0, \quad \forall (\mu \rightarrow \nu) \in G. \quad (14)$$

As noted in [25, 26], this equation is satisfied if the consistency condition between parent-child regions of two marginal probability distributions is satisfied, namely

$$\sum_{\underline{\sigma}_\mu \setminus \underline{\sigma}_\nu} \omega_\mu(\underline{\sigma}_\mu) = \omega_\nu(\underline{\sigma}_\nu), \quad (15)$$

where ω_μ is a Boltzmann factor

$$\omega_\alpha(\underline{\sigma}_\alpha) \equiv \frac{1}{z_\alpha} \prod_{i \in \alpha} \psi_i(\sigma_i) \prod_{a \in \alpha} \psi_a(\underline{\sigma}_{\partial a}) \prod_{\{\mu \rightarrow \nu : \mu \in B_\alpha, \nu \in I_\alpha\}} m_{\mu \rightarrow \nu}(\underline{\sigma}_\nu) \quad (16)$$

and z_α is a normalization factor associated to the region α . Equation (15) ensures that the marginal probability distribution $\omega_\mu(\underline{\sigma}_\mu)$ and $\omega_\nu(\underline{\sigma}_\nu)$ of each parent-to-child pair come from the same joint probability distribution. The constraints on the marginals, together with (16), lead to the generalized belief-propagation equation on each directed edge $\mu \rightarrow \nu$ of the region graph R

$$\prod_{\substack{\alpha \rightarrow \gamma : \\ \{\alpha \in B_\gamma \cap I_\alpha, \gamma \in I_\alpha\}}} m_{\alpha \rightarrow \gamma}(\underline{\sigma}_\gamma) = C \sum_{\underline{\sigma}_\alpha \setminus \underline{\sigma}_\gamma} \prod_{j \in \alpha \setminus \gamma} \psi_j(\sigma_j) \prod_{b \in \alpha \setminus \gamma} \psi_b(\underline{\sigma}_{\partial b}) \prod_{\substack{\{\eta \rightarrow \tau : \\ \eta \in B_\alpha, \tau \in I_\alpha \setminus I_\gamma\}}} m_{\eta \rightarrow \tau}(\underline{\sigma}_\tau) \quad (17)$$

where C is a normalization constant determined by $\sum_{\underline{\sigma}_\nu} m_{\mu \rightarrow \nu}(\underline{\sigma}_\nu) = 1$.

A. Plaquette-rod-vertex region graph description

As a concrete example and as a reference for the following sections, we present explicitly the expression of the Kikuchi partition function (free energy) and the corresponding generalized belief propagation equations for a region graph description of the 2D Edward-Anderson model. Letting now Greek letter α stand for plaquettes, a for rods and i for vertices and introducing auxiliary functions

$$Z_\alpha = \sum_{\underline{\sigma}_\alpha} \prod_{i \in \alpha} \psi_i(\sigma_i) \prod_{a \in \alpha} \psi_a(\underline{\sigma}_{\partial a}) \prod_{\{\mu \rightarrow \nu\}} \prod_{\mu \in B_\alpha, \nu \in I_\alpha} m_{\mu \rightarrow \nu}(\underline{\sigma}_\nu) \quad (18)$$

$$Z_a = \sum_{\underline{\sigma}_a} \psi_a(\underline{\sigma}_{\partial a}) \prod_{i \in a} \psi_i(\sigma_i) \prod_{\{\mu \rightarrow \nu\}} \prod_{\mu \in B_a, \nu \in I_a} m_{\mu \rightarrow \nu}(\underline{\sigma}_\nu) \quad (19)$$

$$Z_i = \sum_{\sigma_i} \psi_i(\sigma_i) \prod_{\{\mu \rightarrow i\}} \prod_{\mu \in B_i} m_{\mu \rightarrow i}(\sigma_i) \quad (20)$$

The Kikuchi partition function (12) can be written compactly as

$$Z_K = e^{-\beta F_K} = \prod_{\alpha \in R} Z_\alpha \prod_{a \in \alpha} Z_a^{-1} \prod_{i \in a} Z_i \quad (21)$$

where each message appears net zero times and F_K refers to the Kikuchi free energy (13). As messages go from parents to children, and as in the chosen region graph we have only parents (plaquettes), children (rods) and grand-children (vertices), we have only two instances of the general equation (17). With reference to Fig. 1, right panel, for the labelling, the first is plaquettes-to-rods and reads

$$\begin{aligned} m_{\alpha \rightarrow a}(\sigma_i, \sigma_j) m_{b \rightarrow i}(\sigma_i) m_{c \rightarrow j}(\sigma_j) &= \frac{1}{Z_{\alpha \rightarrow a}} \sum_{\sigma_l, \sigma_k} \psi_l(\sigma_l) \psi_k(\sigma_k) \psi_b(\sigma_l, \sigma_i) \psi_d(\sigma_l, \sigma_k) \psi_c(\sigma_k, \sigma_j) \\ &\times m_{\rho \rightarrow b}(\sigma_i, \sigma_l) m_{d_1 \rightarrow l}(\sigma_l) m_{d_2 \rightarrow l}(\sigma_l) m_{\eta \rightarrow d}(\sigma_l, \sigma_k) \\ &\times m_{d_3 \rightarrow k}(\sigma_k) m_{d_4 \rightarrow k}(\sigma_k) m_{\lambda \rightarrow c}(\sigma_k, \sigma_j) \end{aligned} \quad (22)$$

where $Z_{\alpha \rightarrow a}$ is a normalization factor. The messages which appear on the LHS of (22) are those depicted with red arrows in Fig 1 (right panel) whereas those on the RHS are depicted blue arrows. Equation (22) can be written compactly, in a form we will use later, as

$$m_{\alpha \rightarrow a}(\underline{\sigma}_a) = \mathcal{F}_{\alpha \rightarrow a}(\{m_{\eta \rightarrow \tau}\}_{[\eta \in B_\alpha, \tau \in I_\alpha \setminus I_a]}, \{m_{\beta \rightarrow \gamma}\}_{[\beta \in (B_a \cap I_\alpha) \setminus \alpha, \gamma \in I_a \setminus a]}) \quad (23)$$

The second instance is the rods-to-vertices equation and reads

$$m_{a \rightarrow i}(\sigma_i) = \frac{1}{Z_{a \rightarrow i}} \sum_{\sigma_j} \psi_j(\sigma_j) \psi_a(\sigma_i, \sigma_j) m_{\alpha \rightarrow a}(\sigma_i, \sigma_j) m_{\beta \rightarrow a}(\sigma_i, \sigma_j) m_{c \rightarrow j}(\sigma_j) m_{d_5 \rightarrow j}(\sigma_j) m_{d_6 \rightarrow j}(\sigma_j) \quad (24)$$

where $Z_{a \rightarrow i}$ is a normalization factor. Referring to Fig. 3 (right panel), the messages on the RHS of (24) are those depicted in black whereas the message on the LHS is depicted in white. Similarly to (22), equation (24) can also be written in a compact form as

$$m_{a \rightarrow i}(\sigma_i) = \mathcal{F}_{a \rightarrow i}(\{m_{\eta \rightarrow \tau}\}_{[\eta \in B_a, \tau \in I_a \setminus I_i]}) \quad (25)$$

The GBP equations (22) and (24) have a somewhat abstract flavor. In practice they should be considered as iterative equations for the real parameters describing the various probability distributions. For completeness we give such a more detailed description in Appendix C below. The region graph shown in Fig. 1 is redundant in the sense that there are two directed paths from a plaquette region α to each of its four vertex child regions [25]. Because of this redundancy the LHS of the GBP equation (22) is a product of three messages, which leads to practical complications in updating the plaquette-to-rod message $m_{\alpha \rightarrow a}(\sigma_i, \sigma_j)$. In general we regard a region graph as a non-redundant region graph if there is at most one directed path from any region to any another region, otherwise the region graph is regarded as redundant [25]. In the case of a non-redundant region graph the GBP equation can be much simplified and the LHS of each GBP equation contains only one message (see [25] for detailed discussions). Although redundant region graphs bring in computational complications, the main reason to prefer redundant region graphs over non-redundant ones is that, in a redundant region graph, more consistency constraints are enforced on the parent-to-child messages and consequently the results are more accurate.

IV. ONE-STEP REPLICA SYMMETRY BREAKING GBP EQUATIONS

We here take up the approach discussed in the Introduction and consider a second-order statistical model built on a second order (1RSB) partition function (1). In the picture we want to consider here the exact free energy could potentially have a large number of metastable states [1, 2]. The Gibbs measure is, in principle, not anymore a pure states but rather decomposes in a convex linear combination of pure states. We assume that in each metastable state k GBP equations (17) are satisfied and we denote with $\{m_{\mu \rightarrow \nu}^{(k)}\}$ the set of their solution, for every $\mu \rightarrow \nu \in R$. Then a Kikuchi approximation of the generalized free energy (1) is given by replacing the exact free energy of every metastable state by the Kikuchi free energy computed at the same metastable state, i.e. $N f_k \rightarrow F_K \{m_{\mu \rightarrow \nu}^{(k)}\}$ in (1). The resulting second-order statistical model is defined as a sum over fixed points of GBP weighted by their respective Kikuchi free energy:

$$\Xi(y) = \sum_k e^{-\beta y N f_k} \simeq \sum_{k \in E} e^{-\beta y F_K \{m_{\mu \rightarrow \nu}^{(k)}\}} \equiv \Xi_K(y), \quad (26)$$

where E denotes the set of GBP fixed points and with Ξ_K we define the Kikuchi approximation of the replicated or second order partition function. By standard folklore we expect either GBP to have only one fixed point, in which case the sum and the additional parameter y in (26) gives no new information, or to have many fixed points, in which case their relative contributions to the sum are controlled by y . The messages $m_{\mu \rightarrow \nu}$ are considered variables in a statistical model, and the restrictions that the messages are fixed points of GBP are interpreted as hard-core constraints

$$\Xi_K = \sum_{k \in E} e^{-\beta y F_K \{m_{\mu \rightarrow \nu}^{(k)}\}} = \sum_{k \in E} \int \mathcal{D}m_{\mu \rightarrow \nu} e^{-\beta y F_K \{m_{\mu \rightarrow \nu}\}} \prod_{\langle \mu \rightarrow \nu \rangle} \delta[m_{\mu \rightarrow \nu} - m_{\mu \rightarrow \nu}^{(k)}] \quad (27)$$

where on each pair of connected region $\langle \mu \rightarrow \nu \rangle$ we have a message $m_{\mu \rightarrow \nu}$ and delta functions enforce (17). By using the GBP constraints like those in (23) and (25), equation (27) can be rewritten as

$$\Xi_K(y) = \int \mathcal{D}m_{\mu \rightarrow \nu} e^{-\beta y F_K \{m_{\mu \rightarrow \nu}\}} \prod_{\langle \mu \rightarrow \nu \rangle} \delta[m_{\mu \rightarrow \nu} - \mathcal{F}_{\mu \rightarrow \nu}(\hat{m})] \quad (28)$$

where \hat{m} briefly indicates all the dependencies of the function \mathcal{F} from the messages involved in the GBP equations. By postulating (28) we have ignored Jacobians from integration of the delta functions. If we insist that $\Xi(y)$ in (26) is only a sum over fixed points, with no pre-factors, we should more properly have

$$\Xi_K(y) = \int \mathcal{D}m_{\mu \rightarrow \nu} e^{-\beta y F_K \{m_{\mu \rightarrow \nu}\}} \left(\prod_{\langle \mu \rightarrow \nu \rangle} \delta[m_{\mu \rightarrow \nu} - \mathcal{F}_{\mu \rightarrow \nu}(\hat{m})] \right) \left| \det \left[\frac{\partial(m_{\mu \rightarrow \nu} - \mathcal{F}_{\mu \rightarrow \nu})}{\partial m_{\mu' \rightarrow \nu'}} \right] \right| \quad (29)$$

where the determinant is of an $L \times L$ matrix with L the number of parent-to-child links in the region graph. This determinant should approximately be $\Lambda_+^{N_+}$ where N_+ is the number of its eigenvalues larger than one and Λ_+ is their geometric mean. The version of (26) given in (1) is in terms of free energy densities, and therefore only up to leading order in N . Hence, the determinant can be ignored if N_+ is sub-linear in N . We will assume that this is so, noting however that the spectra of linearized Belief Propagation (or linearized Generalized Belief Propagation) operators has not, to our knowledge, been systematically investigated in the literature.

Using (21) and (28) we can then write

$$\Xi_K = \sum_{k \in E} e^{-\beta y F_K \{m_{\mu \rightarrow \nu}^{(k)}\}} = \int \mathcal{D}m_{\mu \rightarrow \nu} \prod_{\alpha \in R} Z_\alpha^y \prod_{a \in R} Z_a^{-y} \prod_{i \in R} Z_i^y \prod_{\langle \mu \rightarrow \nu \rangle} \delta[m_{\mu \rightarrow \nu} - \mathcal{F}_{\mu \rightarrow \nu}(\hat{m})] \quad (30)$$

where we recall that Z_α , Z_a and Z_i are functions of the messages as given in (18), (19) and (20). We interpret equation (30) as the partition function of a new model where the messages represent the new variables, the Z 's represent new potential functions, and the delta functions represent new constraints.

A. Higher-level region graph and second-level GBP

The first step towards 1RSB GBP equations is to introduce an auxiliary graphical model where variable nodes contain the messages and factor nodes contain potential functions or constraints. Each factor node is connected to all the variable nodes on which it depends *i.e.* for a potential functions to all the arguments of respectively Z_α , Z_a and Z_i , and for a constraint $\delta[m_{\mu \rightarrow \nu} - \mathcal{F}_{\mu \rightarrow \nu}(\hat{m})]$ both to $m_{\mu \rightarrow \nu}$ and to all the arguments of $\mathcal{F}_{\mu \rightarrow \nu}$. This auxiliary model is a graph expansion of the original model, as discussed for the case of BP in [1].

The second step is to define new regions in the auxiliary graph and assign the second-level potential functions and constraints to these regions. How to do so is not uniquely defined, no more than in the standard CVM. We here choose a region graph for the auxiliary second-level graphical model which is isomorphic to the region graph for the first-level graphical model. This means that plaquettes, rods and vertices on the first level will be in one-to-one correspondence with regions on the second level which we call by the same names. To a plaquette α on the first-level graph corresponds a second-level region denoted by $\hat{\alpha}$ which contains (i) all messages going to descendants of α from the outside or from the inside *i.e.* $B_\alpha \cup I_\alpha$; (ii) the delta functions enforcing that the messages in I_α satisfy GBP; (iii) the potential function Z_α^y . Similarly, to a rod a on the first-level graph corresponds a second-level region denoted by \hat{a} which contains all messages in $B_a \cup I_a$, the two delta functions enforcing that the messages in I_a satisfy GBP, and Z_a^y . To a vertex i corresponds finally \hat{i} which contains the four messages in B_i , and Z_i^y . The procedure is illustrated in Fig 2. The third step is to carry out CVM on (30) with the regions defined in Fig. 2 and define consistency conditions for marginals between parent-to-child regions similarly to those in (15) for the first-level region graph. The second-level CVM is built on messages in the second-level region graph, which are functions of the messages \vec{m} in the first-level region graph and which we here denote as $Q(\vec{m})$ (probabilities of probabilities) illustrated by black arrows in Fig 2, right panel. Every one of these (second-level) messages goes from a parent to a child region and depends on all the (first-level) messages in the child region. When there is a direct link $\hat{\alpha} \rightarrow \hat{a}$ the $Q_{\hat{\alpha} \rightarrow \hat{a}}$ message depends on all the messages in the region \hat{a} , that is all the messages in $B_a \cup I_a$ in the original graph and so depends on 10 (first-level) messages. When there is a direct link $\hat{a} \rightarrow \hat{i}$ the $Q_{\hat{a} \rightarrow \hat{i}}$ message depends on all the messages in the region \hat{i} , corresponding to the region B_i in the original graph and so includes 4 messages (see Fig 2 for an illustration). We represent these

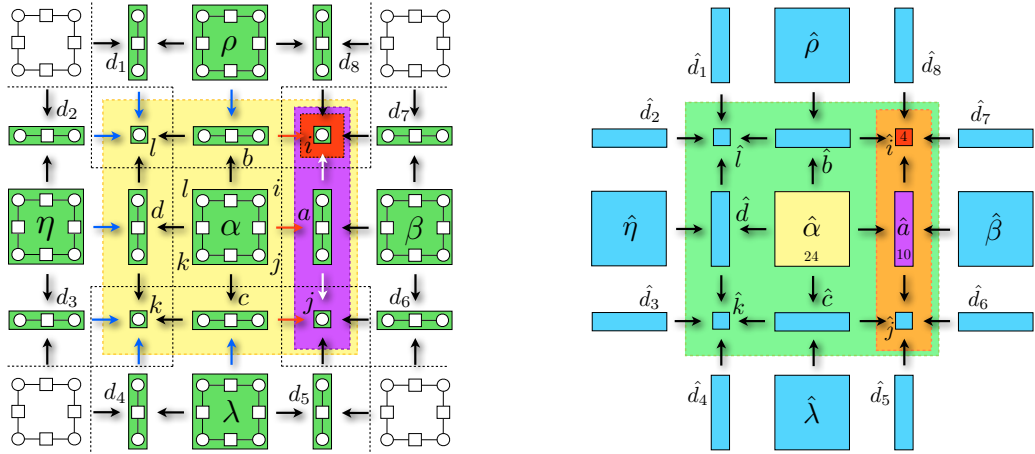


FIG. 2: Left panel: Region graph representation of a 2D EA model in terms of plaquettes, rods and vertices. The border and interior of the plaquette region α is pictured in yellow and becomes the region $\hat{\alpha}$ in the auxiliary model (yellow plaquette in the right panel). The border and interior of the rod region a is pictured in purple and becomes the new rod region \hat{a} (right panel) whereas the border of the vertex region i , which is displayed in red, becomes the new vertex region \hat{i} in the auxiliary model. Right panel: the auxiliary graph in terms of new regions. Numbers inside the regions are a memo of the number of \vec{m} messages contained in each region. The arrows represent the new messages in the auxiliary model, indicated as $Q(\vec{m})$ in the text.

second-level messages in the auxiliary graph as

$$Q_{\hat{\alpha} \rightarrow \hat{a}}(\vec{m}_{\alpha \rightarrow a}^{(2)}, \vec{m}_{a \rightarrow i}^{(8)}) \quad \text{From plaquettes to rods} \quad (31)$$

$$Q_{\hat{a} \rightarrow \hat{i}}(\vec{m}_{a \rightarrow i}^{(4)}) \quad \text{From rods to vertices} \quad (32)$$

where the superscript refers to the number of messages of the kind $\mu \rightarrow \nu$ contained in the argument of Q . That is, the notation $\vec{m}_{\alpha \rightarrow a}^{(l)}$ means l messages of the kind plaquette-to-rod, whereas $\vec{m}_{a \rightarrow i}^{(l)}$ means l messages of the kind rod-to-vertex. In the following, to shorten notation, we omit the labels of the messages \vec{m} when they are arguments of the functions Q , i.e. we simply write $Q_{\hat{\alpha} \rightarrow \hat{a}}(\vec{m}^{(10)})$ and $Q_{\hat{a} \rightarrow \hat{i}}(\vec{m}^{(4)})$.

The messages Q , potential functions Z and constraints in each region now define marginals of the second-level regions respectively denoted $W_{\hat{\alpha}}$, $W_{\hat{a}}$ and $W_{\hat{i}}$, analogously to the marginals (16) in the first-level region graph (see Fig 2). These marginals satisfy the following consistency equations

$$\int_{\hat{\alpha} \setminus \hat{a}} d\vec{m}_{\hat{\alpha}}^{(14)} W_{\hat{\alpha}}(\vec{m}_{\hat{\alpha}}^{(24)}) = W_{\hat{a}}(\vec{m}_{\hat{a}}^{(10)}) \quad \text{For plaquette } \alpha \text{ and rod } a \quad (33)$$

$$\int_{\hat{a} \setminus \hat{i}} d\vec{m}_{\hat{a}}^{(6)} W_{\hat{a}}(\vec{m}_{\hat{a}}^{(10)}) = W_{\hat{i}}(\vec{m}_{\hat{i}}^{(4)}) \quad \text{For rod } a \text{ and vertex } i \quad (34)$$

where the notation $\hat{\alpha} \setminus \hat{a}$ means that the integral is taken over all the messages belonging to $\hat{\alpha}$ except those which are common with \hat{a} (and similarly for $\hat{a} \setminus \hat{i}$) and where with $d\vec{m}_{\hat{\alpha}}$ ($d\vec{m}_{\hat{a}}$) we mean

an integration over the messages contained in the set $\hat{\alpha}$ (\hat{a}). As equations (33) and (34) are the core of our approach to second-level GBP we will write them down explicitly in the following two subsections.

B. Consistency equation for rods and vertices

Following the discussion given in the previous subsection and in analogy with the consistency equations (15), we here write explicitly the consistency equations for the second-level region graph illustrated in Fig. 3. Using a compact notation, the local consistency equation (34) can be written as follows:

$$\frac{1}{\Xi_{\hat{a}}} \int_{\hat{a} \setminus \hat{i}} d\vec{m}_{\hat{a}}^{(6)} Z_a^y \delta_{a \rightarrow i} \delta_{a \rightarrow j} \prod_{(\hat{\mu} \rightarrow \hat{\nu}) \in B(\hat{a})}^{(8)} Q_{\hat{\mu} \rightarrow \hat{\nu}}(\vec{m}^{(10)}) = \frac{1}{\Xi_{\hat{i}}} Z_i^y \prod_{(\hat{b} \rightarrow \hat{i}) \in B(\hat{i})}^{(4)} Q_{\hat{b} \rightarrow \hat{i}}(\vec{m}^{(4)}) \quad (35)$$

where $\Xi_{\hat{a}}$ and $\Xi_{\hat{i}}$ are normalization factors and the superscript on the products indicate how many Q products we have on each side. The delta functions in the equation above enforce the GBP equations (17) for rods-to-vertex messages and are interpreted as hard-core constraints; for short we use the notation $\delta_{\mu \rightarrow \nu} = \delta[m_{\mu \rightarrow \nu} - \mathcal{F}_{\mu \rightarrow \nu}(\hat{m})]$. The Z 's are potential functions referred to the region considered and the Parisi parameter y plays the role of an inverse temperature. Writing more explicitly the above formula for the rod \hat{a} and the vertex \hat{i} on the expanded graph (see Fig. 2) we have

$$\begin{aligned} & \frac{1}{\Xi_{\hat{a}}} \int_{\hat{a} \setminus \hat{i}} d\vec{m}_{\hat{a}}^{(6)} Z_a^y \delta_{a \rightarrow i} \delta_{a \rightarrow j} Q_{\hat{a} \rightarrow \hat{a}}(\vec{m}^{(10)}) Q_{\hat{b} \rightarrow \hat{a}}(\vec{m}^{(10)}) \\ & \quad \underline{Q_{\hat{b} \rightarrow \hat{i}}(\vec{m}^{(4)})} Q_{\hat{d}_8 \rightarrow \hat{i}}(\vec{m}^{(4)}) \underline{Q_{\hat{d}_7 \rightarrow \hat{i}}(\vec{m}^{(4)})} Q_{\hat{c} \rightarrow \hat{j}}(\vec{m}^{(4)}) Q_{\hat{d}_5 \rightarrow \hat{j}}(\vec{m}^{(4)}) Q_{\hat{d}_6 \rightarrow \hat{j}}(\vec{m}^{(4)}) \\ & = \frac{1}{\Xi_{\hat{i}}} Z_i^y Q_{\hat{a} \rightarrow \hat{i}}(\vec{m}^{(4)}) \underline{Q_{\hat{b} \rightarrow \hat{i}}(\vec{m}^{(4)})} Q_{\hat{d}_8 \rightarrow \hat{i}}(\vec{m}^{(4)}) \underline{Q_{\hat{d}_7 \rightarrow \hat{i}}(\vec{m}^{(4)})} \end{aligned} \quad (36)$$

where the common terms in the LHS and RHS have been underlined by a dashed line. Let us observe that, the integration does not involve the underlined terms, indeed referring to Figure 3, central panel, the integration on $\hat{a} \setminus \hat{i}$ involves only the blue \vec{m} messages in the (purple) region \hat{a} but does not involve the black messages shared with the (red) region \hat{i} . We then observe that the argument of the underlined Q 's in (36) only contain the (black) messages in $\hat{a} \setminus \hat{i}$. Therefore the blue Q 's never depend on the variable of integration and hence cancel on both sides of the equation and we have

$$Q_{\hat{a} \rightarrow \hat{i}} = \frac{\Xi_{\hat{i}}}{\Xi_{\hat{a}}} \int_{\hat{a} \setminus \hat{i}} d\vec{m}_{\hat{a}}^{(6)} Z_a^y \delta_{a \rightarrow i} \delta_{a \rightarrow j} Q_{\hat{a} \rightarrow \hat{a}} Q_{\hat{b} \rightarrow \hat{a}} Q_{\hat{c} \rightarrow \hat{j}} Q_{\hat{d}_5 \rightarrow \hat{j}} Q_{\hat{d}_6 \rightarrow \hat{j}} \quad (37)$$

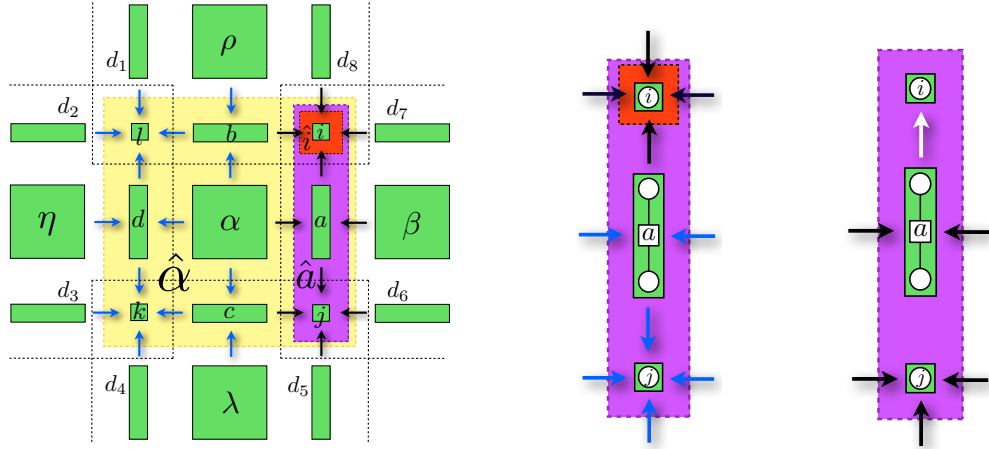


FIG. 3: Left panel: First and second level region graph description overlapped for the 2D EA model. Messages integrated over on the LHS of (33) are illustrated with blue arrows whereas those on the RHS are pictured with black arrows. Central panel: same kind of illustration for equation (34). Right panel: pictorial representation of GBP rod-to-vertex equation (24). The message on the LHS is pictured with a white arrow whereas black arrows illustrate the messages on the RHS.

where we used the relation (A4), i.e. $Z_a/Z_i = Z_{a \rightarrow i}$, and we omitted the dependency from the messages of the Q functions for brevity. Here we can note that $m_{a \rightarrow j}$ is integrated over on RHS and that $Z_{a \rightarrow i}$ does not depend on this message (see (A4) for details) and hence we integrate out this message to obtain

$$Q_{\hat{a} \rightarrow \hat{i}} = \frac{\Xi_{\hat{i}}}{\Xi_{\hat{a}}} \int_{\hat{a} \setminus \hat{i}} d\vec{m}_{\hat{a}}^{(5)} Z_{a \rightarrow i}^y \delta_{a \rightarrow i} \tilde{Q}_{\hat{\alpha} \rightarrow \hat{a}} \tilde{Q}_{\hat{\beta} \rightarrow \hat{a}} \tilde{Q}_{\hat{c} \rightarrow \hat{j}} \tilde{Q}_{\hat{d}_5 \rightarrow \hat{j}} \tilde{Q}_{\hat{d}_6 \rightarrow \hat{j}}. \quad (38)$$

With the tilde notation above we indicated functions Q with the value of $m_{a \rightarrow j}$ in their argument replaced by their GBP updates (25) *i.e.* by $\mathcal{F}_{a \rightarrow j}(\hat{m})$. Equation (38) corresponds to the 1RSB rod-to-vertex Generalized Belief Propagation equation for a 2D lattice model as the EA model and represent the first result of this paper. We remind that the Q and \tilde{Q} functions above are joint probabilities distributions of several messages therefore equation (38), although analytically consistent, it is very hard, perhaps impossible, to iterate numerically. In Section V we discuss how take an SP-like ansatz on the Q functions to allow numerical iterations of the equations.

C. Consistency equation for plaquettes and rods

Similarly to the previous section and with an analogous notation, we here want to write more explicitly the consistency equations between plaquettes and rods on the second-level region graph.

Equation (33) can be written as

$$\frac{1}{\Xi_{\hat{\alpha}}} \int_{\hat{\alpha} \setminus \hat{a}} d\vec{m}^{(14)} Z_{\alpha}^y(\vec{m}) \delta_{\alpha \rightarrow a}^{(4)} \delta_{a \rightarrow i}^{(8)} \prod_{\substack{(\hat{\gamma} \rightarrow \hat{g}) \\ \in B(\hat{\alpha})}}^{(12)} Q_{\hat{\gamma} \rightarrow \hat{g}}(\vec{m}^{(10)}) = \frac{1}{\Xi_{\hat{a}}} Z_a^y(\vec{m}) \delta_{a \rightarrow i} \delta_{a \rightarrow j} \prod_{\substack{(\hat{\mu} \rightarrow \hat{\nu}) \\ \in B(\hat{a})}}^{(8)} Q_{\hat{\mu} \rightarrow \hat{\nu}}(\vec{m}^{(10)}) \quad (39)$$

where $\Xi_{\hat{\alpha}}$ and $\Xi_{\hat{a}}$ are normalization factors. Delta functions in the equation above enforce GBP equations (17) for the messages \vec{m} at both the plaquette-to-rod and rod-to-vertex level and, as for (35), are interpreted as hard-core constraint for the second-level region graph model. Their upper script refers to how many delta functions of the type $\mu \rightarrow \nu$ are included, i.e. on the LHS of (39) four deltas refer to messages from plaquettes to rods ($\delta_{\alpha \rightarrow a}$) and eight deltas to messages from rods to vertices ($\delta_{a \rightarrow i}$). These delta functions, as mentioned, enforce GBP condition on the \vec{m} messages illustrated in the left panel of Figure 2 as blue and white arrows in the interior of the (yellow) region $\hat{\alpha}$; whereas the deltas on the RHS enforce GBP conditions on the \vec{m} messages depicted as the two white arrows in the interior of the (purple) region \hat{a} . Writing the above equation more explicitly we get:

$$\begin{aligned} & \frac{1}{\Xi_{\hat{\alpha}}} \int_{\hat{\alpha} \setminus \hat{a}} d\vec{m}^{(14)} Z_{\alpha}^y(\vec{m}) [\delta_{\alpha \rightarrow a} \delta_{\alpha \rightarrow b} \delta_{\alpha \rightarrow c} \delta_{\alpha \rightarrow d}] [\delta_{a \rightarrow i} \delta_{a \rightarrow j} \delta_{c \rightarrow j} \delta_{c \rightarrow k} \delta_{d \rightarrow k} \delta_{d \rightarrow l} \delta_{b \rightarrow l} \delta_{b \rightarrow i}] \\ & \times \prod_{(\hat{\gamma} \rightarrow \hat{g}) \in B(\hat{\alpha})}^{(4)} Q_{\hat{\gamma} \rightarrow \hat{g}}(\vec{m}^{(10)}) \prod_{(\hat{g} \rightarrow \hat{i}) \in B(\hat{\alpha})}^{(8)} Q_{\hat{g} \rightarrow \hat{i}}(\vec{m}^{(4)}) \\ & = \frac{1}{\Xi_{\hat{a}}} Z_a^y(\vec{m}) \delta_{a \rightarrow i} \delta_{a \rightarrow j} \prod_{\substack{(\hat{\mu} \rightarrow \hat{\nu}) \\ \in B(\hat{a})}}^{(2)} Q_{\hat{\mu} \rightarrow \hat{a}}(\vec{m}^{(10)}) \prod_{\substack{(\hat{b} \rightarrow \hat{l}) \\ \in B(\hat{a})}}^{(6)} Q_{\hat{b} \rightarrow \hat{l}}(\vec{m}^{(4)}) \end{aligned} \quad (40)$$

where, on both side of the equation, we separated the product of the Q messages in those directed to rods and those directed to vertices on the second-level region graph. Writing (40) yet more explicitly we obtain:

$$\begin{aligned} & \frac{\Xi_{\hat{a}}}{\Xi_{\hat{\alpha}}} \int_{\hat{\alpha} \setminus \hat{a}} d\vec{m}^{(14)} \left(\frac{Z_{\alpha}}{Z_a} \right)^y [\delta_{\alpha \rightarrow a} \delta_{\alpha \rightarrow b} \delta_{\alpha \rightarrow c} \delta_{\alpha \rightarrow d}] [\delta_{a \rightarrow i} \delta_{a \rightarrow j} \delta_{c \rightarrow j} \delta_{c \rightarrow k} \delta_{d \rightarrow k} \delta_{d \rightarrow l} \delta_{b \rightarrow l} \delta_{b \rightarrow i}] \\ & \underbrace{Q_{\hat{\beta} \rightarrow \hat{a}}}_{\text{---}} \underbrace{Q_{\hat{\lambda} \rightarrow \hat{c}}}_{\text{---}} \underbrace{Q_{\hat{\eta} \rightarrow \hat{d}}}_{\text{---}} \underbrace{Q_{\hat{\rho} \rightarrow \hat{b}}}_{\text{---}} \underbrace{Q_{\hat{d}_1 \rightarrow \hat{l}}}_{\text{---}} \underbrace{Q_{\hat{d}_2 \rightarrow \hat{l}}}_{\text{---}} \underbrace{Q_{\hat{d}_3 \rightarrow \hat{k}}}_{\text{---}} \underbrace{Q_{\hat{d}_4 \rightarrow \hat{k}}}_{\text{---}} \underbrace{Q_{\hat{d}_5 \rightarrow \hat{j}}}_{\text{---}} \underbrace{Q_{\hat{d}_6 \rightarrow \hat{j}}}_{\text{---}} \underbrace{Q_{\hat{d}_7 \rightarrow \hat{i}}}_{\text{---}} \underbrace{Q_{\hat{d}_8 \rightarrow \hat{i}}}_{\text{---}} \\ & = \delta_{a \rightarrow i} \delta_{a \rightarrow j} \underbrace{Q_{\hat{\alpha} \rightarrow \hat{a}}}_{\text{---}} \underbrace{Q_{\hat{\beta} \rightarrow \hat{a}}}_{\text{---}} \underbrace{Q_{\hat{d}_5 \rightarrow \hat{j}}}_{\text{---}} \underbrace{Q_{\hat{d}_6 \rightarrow \hat{j}}}_{\text{---}} \underbrace{Q_{\hat{d}_7 \rightarrow \hat{i}}}_{\text{---}} \underbrace{Q_{\hat{b} \rightarrow \hat{i}}}_{\text{---}} \underbrace{Q_{\hat{c} \rightarrow \hat{j}}}_{\text{---}}, \end{aligned} \quad (41)$$

where the common terms in the LHS and RHS have been underlined with dashed lines for clearness and we moved the normalization factors and potential functions to LHS. Note that, as in the previous section, the integration does not involve the underlined terms, indeed referring to Figure

3, left panel, the integration on $\hat{\alpha} \setminus \hat{a}$ involves only the blue messages in the (yellow) region $\hat{\alpha}$ but does not involve the black messages shared with the (purple) region \hat{a} . We then observe that the argument of the underlined Q's in (41) only contains the (black) messages in \hat{a} . In addition, also the two underlined deltas only involve the (black) messages in \hat{a} (see Figure 3, right panel) which means that, even when the deltas are enforced, they don't involve any (blue) message from the set $\hat{\alpha} \setminus \hat{a}$ into the remaining variables. Therefore the underlined Q's never depend on the variable of integration and hence cancel on both sides of the equation

$$\frac{\Xi_{\hat{a}}}{\Xi_{\hat{\alpha}}} \int_{\hat{\alpha} \setminus \hat{a}} d\vec{m}^{(14)} Z_{\alpha \rightarrow a}^y(\vec{m}) [\delta_{\alpha \rightarrow a} \delta_{\alpha \rightarrow b} \delta_{\alpha \rightarrow c} \delta_{\alpha \rightarrow d}] [\delta_{a \rightarrow i} \delta_{a \rightarrow j} \delta_{c \rightarrow j} \delta_{c \rightarrow k} \delta_{d \rightarrow k} \delta_{d \rightarrow l} \delta_{b \rightarrow l} \delta_{b \rightarrow i}] Q_{\hat{\lambda} \rightarrow \hat{c}} Q_{\hat{\eta} \rightarrow \hat{d}} Q_{\hat{\rho} \rightarrow \hat{b}} Q_{\hat{d}_1 \rightarrow \hat{l}} Q_{\hat{d}_2 \rightarrow \hat{l}} Q_{\hat{d}_3 \rightarrow \hat{k}} Q_{\hat{d}_4 \rightarrow \hat{k}} = \delta_{a \rightarrow i} \delta_{a \rightarrow j} Q_{\hat{\alpha} \rightarrow \hat{a}} Q_{\hat{b} \rightarrow \hat{i}} Q_{\hat{c} \rightarrow \hat{j}}, \quad (42)$$

where we made use of the relation (A5), i.e. $Z_\alpha / Z_a = Z_{\alpha \rightarrow a}$. The remaining two deltas $\delta_{a \rightarrow i} [m_{a \rightarrow i} - \mathcal{F}_{a \rightarrow i}(\hat{m})]$ and $\delta_{a \rightarrow j} [m_{a \rightarrow j} - \mathcal{F}_{a \rightarrow j}(\hat{m})]$ depend only on messages in \hat{a} , i.e. on first-level messages which are not integrated over in (42). Therefore, although \hat{a} contains ten messages equation (42) only holds information for the subset where the two messages $m_{a \rightarrow i}$ and $m_{a \rightarrow j}$ in I_a are determined by the eight messages in B_a through the constraints $\delta_{a \rightarrow i}$ and $\delta_{a \rightarrow j}$. Otherwise the meaning of (42) is trivially $0 = 0$.

To illustrate this point again we consider what happens if we integrate both sides of (42) over $m_{a \rightarrow i}$ and $m_{a \rightarrow j}$. The messages $m_{a \rightarrow i}$ and $m_{a \rightarrow j}$ appear as arguments of several functions both on the left and right hand side of the equation (42). Hence, wherever they appear, they must be substituted with the GBP equations enforced by the two deltas, which, as noted above, never involve (blue) message from the set $\hat{\alpha} \setminus \hat{a}$. Then the effect of the integration over these two messages is just substituting either (the black) $m_{a \rightarrow i}$ or $m_{a \rightarrow j}$ with a function of other (black) messages belonging to the set \hat{a} (see Figure 3). More specifically, the message $m_{a \rightarrow i}$ appears on the LHS of (42) in the GBP delta constraint $\delta_{b \rightarrow l} (m_{b \rightarrow l} - F_{b \rightarrow l} (m_{\rho \rightarrow b}, m_{\alpha \rightarrow b}, m_{\rho \rightarrow b}, \underline{m_{a \rightarrow i}}, m_{d_7 \rightarrow i}, m_{d_8 \rightarrow i}))$ and similarly in $\delta_{\alpha \rightarrow b}$. It also appears as argument of the Q functions $Q_{\rho \rightarrow b}$ on the LHS and $Q_{\alpha \rightarrow a}$ and $Q_{b \rightarrow i}$ on the RHS. Likewise, the message $m_{a \rightarrow j}$ appears as argument on the LHS in $\delta_{c \rightarrow k}, \delta_{\alpha \rightarrow c}, Q_{\lambda \rightarrow c}$ and in $Q_{\alpha \rightarrow a}, Q_{c \rightarrow j}$ on the RHS. The result after the integration over $m_{a \rightarrow i}$ and $m_{a \rightarrow j}$ is therefore the following:

$$\tilde{Q}_{\hat{\alpha} \rightarrow \hat{a}} \tilde{Q}_{\hat{b} \rightarrow \hat{i}} \tilde{Q}_{\hat{c} \rightarrow \hat{j}} = \frac{\Xi_{\hat{a}}}{\Xi_{\hat{\alpha}}} \int_{\hat{\alpha} \setminus \hat{a}} d\vec{m}^{(14)} Z_{\alpha \rightarrow a}^y [\delta_{\alpha \rightarrow a} \tilde{\delta}_{\alpha \rightarrow b} \tilde{\delta}_{\alpha \rightarrow c} \delta_{\alpha \rightarrow d}] [\delta_{c \rightarrow j} \tilde{\delta}_{c \rightarrow k} \delta_{d \rightarrow k} \delta_{d \rightarrow l} \tilde{\delta}_{b \rightarrow l} \delta_{b \rightarrow i}] \tilde{Q}_{\hat{\lambda} \rightarrow \hat{c}} \tilde{Q}_{\hat{\eta} \rightarrow \hat{d}} \tilde{Q}_{\hat{\rho} \rightarrow \hat{b}} Q_{\hat{d}_1 \rightarrow \hat{l}} Q_{\hat{d}_2 \rightarrow \hat{l}} Q_{\hat{d}_3 \rightarrow \hat{k}} Q_{\hat{d}_4 \rightarrow \hat{k}} \quad (43)$$

where now \tilde{Q} ($\tilde{\delta}$) are the functions Q (δ) with the value of $m_{a \rightarrow i}$ and $m_{a \rightarrow j}$ in their argument replaced by their GBP updates i.e. by $\mathcal{F}_{a \rightarrow i}(\dots)$ and $\mathcal{F}_{a \rightarrow j}(\dots)$, as for the previous section. Note

that this last integration of these two deltas carried some of the dependence on the black messages into the functions Q on the RHS. Equation (43) corresponds to the 1RSB plaquette-to-rod GBP equation for the 2D EA model. Since the Q 's functions above are joint probability distribution of messages, similar considerations as those in the text below (38) apply here.

V. ABSENCE OF GENERALIZED SURVEY PROPAGATION

We start by explaining the approach to Survey Propagation (SP) described in [1], an argument which in fact also works for our rod-to-vertex equations (37).

The success of Belief Propagation is to a large extent due to its moving information forward. Indeed, this is why these algorithms are referred to as propagation. SP is a special class of solutions to the general second-level, 1RSB, BP equations which has the same property and for which the fixed points can therefore be found by forward iteration. In the following we want to verify whether the second-level 1RSB GBP equations presented in the previous section admit a special class of solutions of the SP-type and can therefore be written as Generalized Survey Propagation equations. The special solutions of SP are derived by assuming that a second-level message $Q_{\hat{a} \rightarrow \hat{i}}$ only depends on the one first-level message going the same way, *i.e.* on $m_{a \rightarrow i}$. Following the SP ansatz we assume that this is so for all messages on RHS of (37). Then the message $m_{a \rightarrow j}$ only appears on RHS as an argument of the delta function $\delta_{a \rightarrow j}$, and can be integrated out to give

$$Q_{\hat{a} \rightarrow \hat{i}}(m_{a \rightarrow i}, m_{b \rightarrow i}, m_{d_8 \rightarrow i}, m_{d_7 \rightarrow i}) = \frac{\Xi_{\hat{i}}}{\Xi_{\hat{a}}} \int_{\hat{a} \setminus \hat{i}} d\vec{m}_{\hat{a}}^{(5)} Z_{a \rightarrow i}^y[m_{\alpha \rightarrow a}, m_{\beta \rightarrow a} m_{c \rightarrow j}, m_{d_5 \rightarrow j}, m_{d_6 \rightarrow j}] \times \delta_{a \rightarrow i}[m_{a \rightarrow i} - \mathcal{F}_{a \rightarrow i}] Q_{\hat{a} \rightarrow \hat{a}} Q_{\hat{\beta} \rightarrow \hat{a}} Q_{\hat{c} \rightarrow \hat{j}} Q_{\hat{d}_5 \rightarrow \hat{j}} Q_{\hat{d}_6 \rightarrow \hat{j}} \quad (44)$$

where we have written out the arguments of $Q_{\hat{a} \rightarrow \hat{i}}$ (on LHS) and $Z_{a \rightarrow i}$ (on RHS) explicitly. Compared to (38) we have now gained that the Q functions appearing on RHS are the original Q 's, which by assumption still only depend on one underlying first-level message. Let us now consider on what arguments actually depends $Q_{\hat{a} \rightarrow \hat{i}}$. Obviously it depends on its first argument since $m_{a \rightarrow i}$ appears explicitly on RHS. However, it does not depend on its other three arguments since neither $m_{b \rightarrow i}$ nor $m_{d_8 \rightarrow i}$ nor $m_{d_7 \rightarrow i}$ appear on RHS. Therefore the assumption that second-level messages only depend on the underlying first-level message going the same way is preserved by the iteration of (44).

The problem arises when we want to do the same thing for the plaquettes-to-rods equation (42).

Let us for convenience include it here again as

$$\begin{aligned}
Q_{\hat{\alpha} \rightarrow \hat{a}} Q_{\hat{b} \rightarrow \hat{i}} Q_{\hat{c} \rightarrow \hat{j}} &= \frac{\Xi_{\hat{a}}}{\Xi_{\hat{\alpha}}} \int_{\hat{\alpha} \setminus \hat{a}} d\vec{m}^{(14)} Z_{\alpha \rightarrow a}^y [m_{\rho \rightarrow b}, m_{\eta \rightarrow d}, m_{\lambda \rightarrow c}, m_{d_1 \rightarrow j}, m_{d_2 \rightarrow j}, m_{d_3 \rightarrow k}, m_{d_4 \rightarrow k}] \\
&\times [\underline{\delta_{\alpha \rightarrow a}} \delta_{\alpha \rightarrow b} \delta_{\alpha \rightarrow c} \delta_{\alpha \rightarrow d}] [\underline{\delta_{c \rightarrow j}} \delta_{c \rightarrow k} \delta_{d \rightarrow k} \delta_{d \rightarrow l} \delta_{b \rightarrow l} \underline{\delta_{b \rightarrow i}}] \\
&\times Q_{\hat{\lambda} \rightarrow \hat{c}} Q_{\hat{\eta} \rightarrow \hat{d}} Q_{\hat{\rho} \rightarrow \hat{b}} Q_{\hat{d}_1 \rightarrow \hat{l}} Q_{\hat{d}_2 \rightarrow \hat{l}} Q_{\hat{d}_3 \rightarrow \hat{k}} Q_{\hat{d}_4 \rightarrow \hat{k}}
\end{aligned} \tag{45}$$

where for simplicity we suppressed the constraints $\delta_{a \rightarrow i}$ and $\delta_{a \rightarrow j}$ on both sides (contrary to (43) we do not assume that they have been integrated out, and the delta functions on RHS are hence all the original deltas). The underlined deltas in (45) refer to forward propagation and an argument which is not integrated over while the non-underlined deltas refer to messages in $\hat{\alpha} \setminus \hat{a}$. We can assume that $Q_{\hat{b} \rightarrow \hat{i}}$ and $Q_{\hat{c} \rightarrow \hat{j}}$ have been determined by (44) and therefore only depend on the first-level messages $m_{b \rightarrow i}$ and $m_{c \rightarrow j}$, and we also assume that all Q 's on RHS of (45) only depend on their underlying first-level messages.

The question is then: on what depends $Q_{\hat{\alpha} \rightarrow \hat{a}}$? In principle it could depend on all first-level messages in \hat{a} while we would like it to depend only on $m_{\alpha \rightarrow a}$. Let us consider one of the other messages in \hat{a} , the oppositely directed plaquette-to-rod message $m_{\beta \rightarrow a}$. This message is not an argument $Z_{\alpha \rightarrow a}$ nor does, by assumption, any of the Q 's on RHS of (45) depend on it. However, the three deltas $\delta_{\alpha \rightarrow b}$, $\delta_{\alpha \rightarrow c}$ and $\delta_{\alpha \rightarrow d}$ do depend on $m_{\beta \rightarrow a}$ through the GBP update functions $\mathcal{F}_{\alpha \rightarrow b}$, $\mathcal{F}_{\alpha \rightarrow c}$ and $\mathcal{F}_{\alpha \rightarrow d}$. Therefore, if we integrate over internal variables $m_{\alpha \rightarrow b}$, $m_{\alpha \rightarrow c}$ and $m_{\alpha \rightarrow d}$ the dependence on $m_{\beta \rightarrow a}$ is transferred to the two underlined rod-to-vertices deltas $\tilde{\delta}_{c \rightarrow j}$ and $\tilde{\delta}_{b \rightarrow i}$, and to the four rod-to-vertices deltas $\tilde{\delta}_{c \rightarrow k}$, $\tilde{\delta}_{d \rightarrow k}$, $\tilde{\delta}_{d \rightarrow l}$ and $\tilde{\delta}_{b \rightarrow l}$ (and which are all therefore given the tilde mark). We note that $\delta_{\alpha \rightarrow a}$ only depends on $m_{\alpha \rightarrow a}$ and some messages in $B_{\hat{\alpha}}$ and is therefore not changed by this operation. We further note that $m_{\beta \rightarrow a}$ enters in the constraints $\delta_{a \rightarrow i}$ and $\delta_{a \rightarrow j}$ which we have suppressed, but as the arguments of these are assumed constant this is no restriction. For given values of the external messages in $B_{\hat{\alpha}}$ RHS of (45) depends on $m_{\beta \rightarrow a}$ and therefore we conclude that the ansatz that every second-level message $Q_{\mu \rightarrow \nu}$ only depends on its underlying first-level message $m_{\mu \rightarrow \nu}$ is not preserved by the plaquette-to-rod equation (45).

VI. DISCUSSION

We have considered a one-step replica symmetry breaking description of the Edwards-Anderson model in 2D through a second-level statistical model built on the extremal points of a Kikuchi approximation. We have shown that such a theory can be constructed and expressed as consistency equations between marginals of probabilities on probabilities and this brings to 1RSB GBP

equations. Such equations though do not have simple solutions analogous to Survey Propagation. Therefore, although the consistency equations can be written explicitly they are not likely to be solvable by forward iteration *i.e.* as a “propagation”. We believe in fact this to be a general phenomenon. On a graph in finite dimension and with short loops, both the first-level consistency equations *i.e.* “General Belief Propagation” and the second-level 1RSB consistency equations, which we have introduced here, move information around the loops in the region graphs defining the model. On a locally tree-like graph, where these loops are long, two counter-propagating messages diverge from each other and essentially never meet again: it is therefore natural that a second-level model should have a solution where it is never aware of a counter-propagating message. However, in the kind of models which we have considered here, where there are many short loops, – of length four and above, as can easily be checked – two counter-propagating messages can meet soon again, and for a second-level model to have a propagating solution means a number of additional constraints that do not need to have a solution.

One can speculate that the conceptual difference uncovered here between a 1RSB description of a Bethe vs a Kikuchi approximation says something about the physics of spin glass models in finite dimensions.

VII. ACKNOWLEDGMENTS

The authors thank Federico Ricci-Tersenghi for valuable discussions. This research is supported by FP7/2007-2013/grant agreement no 290038 (GDF), by the Swedish Science Council through grant 621-2012-2982 (EA), by the Academy of Finland through its Center of Excellence COIN (EA), and by the Natural Science Foundation of China through grant 11225526 (HJZ). GDF and EA thank the hospitality of KITPC and HJZ thanks the hospitality of KTH.

Appendix A: Useful relations relative to the the partition functions

In this appendix we want to show some relations among the different partition functions encountered in the main text which are useful for the presentation of the theory in Sec IV. We wish to show that the partition functions which appear as normalizing constant in the GBP equations (22) and (24) can be written as rate among two region-graph partition functions introduced in

(18), (19) and (20). Let us write explicitly these latter equations:

$$Z_\alpha = \sum_{\sigma_i, \sigma_j, \sigma_k, \sigma_l} \psi_i(\sigma_i) \psi_j(\sigma_j) \psi_k(\sigma_k) \psi_l(\sigma_l) \psi_a(\sigma_i, \sigma_j) \psi_b(\sigma_l, \sigma_i) \psi_c(\sigma_j, \sigma_k) \psi_d(\sigma_k, \sigma_l) \\ \times m_{\beta \rightarrow a}(\sigma_i, \sigma_j) m_{\rho \rightarrow b}(\sigma_l, \sigma_i) m_{\eta \rightarrow d}(\sigma_k, \sigma_l) m_{\lambda \rightarrow c}(\sigma_j, \sigma_k) \\ \times m_{d_1 \rightarrow l}(\sigma_l) m_{d_2 \rightarrow l}(\sigma_l) m_{d_3 \rightarrow k}(\sigma_k) m_{d_4 \rightarrow k}(\sigma_k) m_{d_5 \rightarrow j}(\sigma_j) m_{d_6 \rightarrow j}(\sigma_j) m_{d_7 \rightarrow i}(\sigma_i) m_{d_8 \rightarrow i}(\sigma_i) \quad (\text{A1})$$

$$Z_a = \sum_{\sigma_i, \sigma_j} \psi_i(\sigma_i) \psi_j(\sigma_j) \psi_a(\sigma_i, \sigma_j) m_{\alpha \rightarrow a}(\sigma_i, \sigma_j) m_{\beta \rightarrow a}(\sigma_i, \sigma_j) \\ \times m_{b \rightarrow i}(\sigma_i) m_{d_8 \rightarrow i}(\sigma_i) m_{d_7 \rightarrow i}(\sigma_i) m_{c \rightarrow j}(\sigma_j) m_{d_5 \rightarrow j}(\sigma_j) m_{d_6 \rightarrow j}(\sigma_j) \quad (\text{A2})$$

$$Z_i = \sum_{\sigma_i} \psi_i(\sigma_i) m_{a \rightarrow i}(\sigma_i) m_{b \rightarrow i}(\sigma_i) m_{d_8 \rightarrow i}(\sigma_i) m_{d_7 \rightarrow i}(\sigma_i) \quad (\text{A3})$$

We want now to show that the rate $Z_\alpha/Z_a = Z_{\alpha \rightarrow a}$, which is the normalization factor in (22) and that $Z_a/Z_i = Z_{a \rightarrow i}$, which is the normalization factor in (24). Explicitly

$$\frac{Z_a}{Z_i} = \frac{\sum_{\sigma_i, \sigma_j} \psi_a \psi_i \psi_j m_{\alpha \rightarrow a} m_{\beta \rightarrow a} m_{b \rightarrow i} m_{d_8 \rightarrow i} m_{d_7 \rightarrow i} m_{c \rightarrow j} m_{d_5 \rightarrow j} m_{d_6 \rightarrow j}}{\sum_{\sigma_i} \psi_i m_{a \rightarrow i} m_{b \rightarrow i} m_{d_8 \rightarrow i} m_{d_7 \rightarrow i}} \\ = \frac{Z_{a \rightarrow i} \sum_{\sigma_i} \psi_i m_{a \rightarrow i} m_{b \rightarrow i} m_{d_8 \rightarrow i} m_{d_7 \rightarrow i}}{\sum_{\sigma_i} \psi_i m_{a \rightarrow i} m_{b \rightarrow i} m_{d_8 \rightarrow i} m_{d_7 \rightarrow i}} = Z_{a \rightarrow i} [m_{\alpha \rightarrow a}, m_{\beta \rightarrow a} m_{c \rightarrow j}, m_{d_5 \rightarrow j}, m_{d_6 \rightarrow j}] \quad (\text{A4})$$

where in the second equality we used the GBP equation (24) to recognize $m_{a \rightarrow i}$ in the numerator. The dependencies of $Z_{a \rightarrow i}$ on the messages are written explicitly on the RHS. Using the expression in (A2) and (A1), a similar calculation shows that the rate Z_α/Z_a is equal to:

$$\frac{Z_\alpha}{Z_a} = Z_{\alpha \rightarrow a} [m_{\rho \rightarrow b}, m_{\eta \rightarrow d}, m_{\lambda \rightarrow c}, m_{d_1 \rightarrow j}, m_{d_2 \rightarrow j}, m_{d_3 \rightarrow k}, m_{d_4 \rightarrow k}] \quad (\text{A5})$$

where we used the GBP equation (22) to substitute terms in the numerator and $Z_{\alpha \rightarrow a}$ represents the corresponding normalization factor with its own dependencies written explicitly for clarity.

Appendix B: A derivation of GBP

In this appendix we derive the GBP update equations (17) from a constrained variation of the Kikuchi free energy functional (8). The material is standard and included only for completeness, see [3]. The task is to minimize the Kikuchi free energy functional F_K in (8) *i.e.*

$$F_K = \sum_{\alpha} c_{\alpha} \sum_{\underline{\alpha}} P_{\alpha}(\underline{\alpha}) \left[E_{\alpha} + \beta^{-1} \log P_{\alpha}(\underline{\alpha}) \right]$$

where we have introduced the energy of a region as

$$E_{\alpha} \sum_{i \in \alpha} h_i \sigma_i + \sum_{a \in \alpha} J_{ij}^{(a)} \sigma_i \sigma_j.$$

The variation is of the marginal probabilities $P_\alpha(\underline{\sigma}_\alpha)$ under the constraints that they all have to come from the same probability distribution. This means, in the situation under consideration, that if a rod region a is a child of plaquette region α then $\sum_{\underline{\sigma}_\alpha \setminus \underline{\sigma}_a} P_\alpha(\underline{\sigma}_\alpha) = P_a(\underline{\sigma}_a)$ where $\underline{\sigma}_\alpha \setminus \underline{\sigma}_a$ is the exclusion set consisting of all spins in α that are not in a . Similarly, if a vertex region i is a child of rod region a then $\sum_{\underline{\sigma}_a \setminus \sigma_i} P_a(\underline{\sigma}_a) = P_i(\sigma_i)$. Introducing Lagrange multipliers $\lambda_{\alpha|a}(\sigma_l, \sigma_k)$ and $\lambda_{a|i}(\sigma_i)$ to represent all these constraints, where the spin indexing follows Fig. 1, as well Lagrange multipliers q_α , q_a and q_i for the normalizations of P_α , P_a and P_i , we arrive at

$$\begin{aligned} P_i &\propto e^{-\beta E_i} e^{\frac{1}{c_i} \beta \sum_{a:a \rightarrow i} \lambda_{a|i}} \\ P_a &\propto e^{-\beta E_a} e^{-\frac{1}{c_a} \beta \sum_{i:a \rightarrow i} \lambda_{a|i}} e^{\frac{1}{c_a} \beta \sum_{\alpha:\alpha \rightarrow a} \lambda_{\alpha|a}} \\ P_\alpha &\propto e^{-\beta E_\alpha} e^{-\frac{1}{c_\alpha} \beta \sum_{a:\alpha \rightarrow a} \lambda_{\alpha|a}} \end{aligned} \quad (\text{B1})$$

Referring to Fig. 1 for the labeling of the regions, where *e.g.* vertex i has four rod parents, of which one is a and the one opposite is called d_8 , and a rod has two plaquette parents, of which one is α and the other one is β , we can introduce auxiliary normalized quantities

$$m_{a \rightarrow i} \propto e^{\beta \lambda_{d_8|i}} \quad (\text{B2})$$

$$m_{\beta \rightarrow a} \propto e^{-\beta \lambda_{\alpha|a} - \lambda_{d_6|j} - \lambda_{d_7|i}} \quad (\text{B3})$$

In terms of the $m_{a \rightarrow i}$ and the $m_{\alpha \rightarrow a}$ the marginal probabilities of the regions then take the GBP output equation form *i.e*

$$\begin{aligned} P_i &\propto e^{-\beta E_i} \prod_{a:a \rightarrow i} m_{a \rightarrow i} \\ P_a &\propto e^{-\beta E_a} m_{\alpha \rightarrow a} m_{\beta \rightarrow a} \prod_{b:b \rightarrow i \setminus a} m_{b \rightarrow i} \prod_{c:c \rightarrow j \setminus a} m_{c \rightarrow j} \\ P_\alpha &\propto e^{-\beta E_\alpha} m_{\beta \rightarrow a} m_{\rho \rightarrow b} m_{\eta \rightarrow d} m_{\lambda \rightarrow c} \prod_{k=1}^8 m_{d_k \rightarrow} \end{aligned} \quad (\text{B4})$$

where the dummy argument in $m_{d_k \rightarrow}$ indicates the vertex in the intersection of d_k and α . Varying the messages in (B4) gives the GBP update equations as described in the main text. Alternatively one can check that the marginalization constraints expressed in the Lagrange multipliers themselves, which are

$$\begin{aligned} e^{-\beta \sum_{b:b \rightarrow i \setminus a} \lambda_{b|i}} &\propto \sum_{\sigma_j} e^{-\beta(E_a - E_i) + \beta \lambda_{a|j} - \beta(\lambda_{\alpha|a} + \lambda_{\beta|a})} \\ e^{\beta(\lambda_{a|i} + \lambda_{a|j}) - \beta \lambda_{\beta|a}} &\propto \sum_{\sigma_l, \sigma_k} e^{-\beta(E_\alpha - E_a) - \beta \sum_{c:\alpha \rightarrow c \setminus a} \lambda_{\alpha|c}} \end{aligned} \quad (\text{B5})$$

are equivalent to the GBP update equations for the messages. We observe that nothing in the above derivation really depends on how many variables (spins) there are in the various regions and what their interactions are; the derivation therefore also holds for the second-level GBP.

Appendix C: GBP equations for the 2D Edwards-Anderson model: from messages to fields.

In this appendix we want to parametrize the messages in equations (22) and (24) in terms of cavity fields and write the correspondent GBP equations for these fields. A message $m_{a \rightarrow i}(\sigma_i)$, which is a probability distribution on the spin σ_i , up to a normalization, can therefore be written $e^{\beta h_{a \rightarrow i}^{(i)} \sigma_i}$ where $h_{a \rightarrow i}^{(i)}$ is a real number known as the cavity bias on spin i from interaction a . Similarly, a message $m_{\alpha \rightarrow a}(\sigma_i, \sigma_j)$ is a probability distribution on two spins σ_i and σ_j and can be written, up to a normalization, as $e^{\beta(h_{\alpha \rightarrow a}^{(i)} \sigma_i + h_{\alpha \rightarrow a}^{(j)} \sigma_j + \kappa_{\alpha \rightarrow a}^{(ij)} \sigma_i \sigma_j)}$ where the new quantity $\kappa_{\alpha \rightarrow a}^{(ij)}$ parametrizes cooperative interactions. The GBP equations (22) and (24) are then to be understood as relations between parameters of the types $h_{a \rightarrow i}^{(i)}$, $h_{\alpha \rightarrow a}^{(i)}$ and $\kappa_{\alpha \rightarrow a}^{(ij)}$. In addition we remind that the potential functions ψ present in the GBP equations are given accordingly to the definition in the EA model as in (4), namely $\psi_i(\sigma_i) = e^{\beta h_i \sigma_i}$ and $\psi_a(\underline{\sigma}_{\partial a}) = e^{\beta J_{ij}^{(a)} \sigma_i \sigma_j}$.

Rod-to-vertex equation: To write this equation explicitly we note that the RHS of (24) can be parametrized as a function of the spin σ_i and σ_j :

$$m_{a \rightarrow i}(\sigma_i) = \frac{1}{Z_{a \rightarrow i}} \exp [\beta h_{a \rightarrow i}^{(i)} \sigma_i] = \frac{1}{Z_{a \rightarrow i}} \sum_{\sigma_j} e^{\beta(x_i \sigma_i + x_j \sigma_j + X_{ij} \sigma_i \sigma_j)}, \quad (\text{C1})$$

where

$$x_i = h_{\alpha \rightarrow a}^{(i)} + h_{\beta \rightarrow a}^{(i)}, \quad (\text{C2})$$

$$x_j = h_j + h_{\alpha \rightarrow a}^{(j)} + h_{\beta \rightarrow a}^{(j)} + h_{c \rightarrow j}^{(j)} + h_{d_5 \rightarrow j}^{(j)} + h_{d_6 \rightarrow j}^{(j)}, \quad (\text{C3})$$

$$X_{ij} = J_{ij}^{(a)} + \kappa_{\alpha \rightarrow a}^{(ij)} + \kappa_{\beta \rightarrow a}^{(ij)}. \quad (\text{C4})$$

Computing the rate $m_{a \rightarrow i}(1)/m_{a \rightarrow i}(-1)$ with the parametrization given above and taking the logarithm on both sides of the resulting equation, we obtain the expression for the rod-to-vertex field:

$$h_{a \rightarrow i}^{(i)} = x_i + \frac{1}{2\beta} \ln \left[\frac{\cosh[\beta(x_j + X_{ij})]}{\cosh[\beta(x_j - X_{ij})]} \right] \quad (\text{C5})$$

Plaquette-to-rod equation: In the following we will not keep track of the normalization constants of the various messages. With the parametrization of messages in terms of fields given above, equation (22) can be written as:

$$\exp \left[\beta \left((h_{\alpha \rightarrow a}^{(i)} + h_{b \rightarrow i}^{(i)}) \sigma_i + (h_{\alpha \rightarrow a}^{(j)} + h_{c \rightarrow j}^{(j)}) \sigma_j + \kappa_{\alpha \rightarrow a}^{(ij)} \sigma_i \sigma_j \right) \right] = K(\sigma_i, \sigma_j) \quad (\text{C6})$$

where the function $K(\sigma_i, \sigma_j)$, according to the RHS of (22), reads as:

$$K(\sigma_i, \sigma_j) = \sum_{\sigma_k, \sigma_l} \exp \left[\left((h_l + h_{\rho \rightarrow l}^{(l)} + h_{d_1 \rightarrow l}^{(l)} + h_{d_2 \rightarrow l}^{(l)} + h_{\eta \rightarrow d}^{(l)}) \sigma_l + h_{\rho \rightarrow b}^{(i)} \sigma_i \right. \right. \quad (C7)$$

$$\left. \left. (h_k + h_{\eta \rightarrow d}^{(k)} + h_{d_3 \rightarrow k}^{(k)} + h_{d_4 \rightarrow k}^{(k)} + h_{\lambda \rightarrow c}^{(k)}) \sigma_k + h_{\lambda \rightarrow c}^{(j)} \sigma_j + \right. \right. \quad (C8)$$

$$\left. \left. (J_{li}^{(b)} + \kappa_{\rho \rightarrow b}^{(li)}) \sigma_l \sigma_i + (J_{lk}^{(d)} + \kappa_{\eta \rightarrow d}^{(lk)}) \sigma_l \sigma_k + (J_{kj}^{(c)} + \kappa_{\lambda \rightarrow c}^{(kj)}) \sigma_k \sigma_j \right) \right]. \quad (C9)$$

After some simple algebra the plaquette-to-rod fields on the LHS of (C6) are then given by

$$h_{\alpha \rightarrow a}^{(i)} = \frac{1}{4\beta} \log \left[\frac{K(1, 1)K(1, -1)}{K(-1, 1)K(-1, -1)} \right] - h_{b \rightarrow i}^{(i)}, \quad (C10)$$

$$h_{\alpha \rightarrow a}^{(j)} = \frac{1}{4\beta} \log \left[\frac{K(1, 1)K(-1, 1)}{K(1, -1)K(-1, -1)} \right] - h_{c \rightarrow j}^{(j)}, \quad (C11)$$

$$\kappa_{\alpha \rightarrow a}^{(ij)} = \frac{1}{4\beta} \log \left[\frac{K(1, 1)K(-1, -1)}{K(1, -1)K(-1, 1)} \right]. \quad (C12)$$

[1] Marc Mézard and Andrea Montanari. *Information, physics, and computation*. Oxford University Press, 2009.

[2] Rémi Monasson. Structural glass transition and the entropy of the metastable states. *Physical review letters*, 75(15):2847, 1995.

[3] Jonathan S Yedidia, William T Freeman, and Yair Weiss. Understanding belief propagation and its generalizations. In *Exploring artificial intelligence in the new millennium*, pages 239–269. Morgan Kaufmann Publishers Inc., 2003.

[4] Martin J. Wainwright and Michael I. Jordan. Graphical models, exponential families, and variational inference. *Foundations and Trends in Machine Learning*, 1:1–305, 2008.

[5] Marc Mézard and Giorgio Parisi. The Bethe lattice spin glass revisited. *Eur. Phys. J. B*, 20(2):217–233, 2001.

[6] Marc Mézard and Riccardo Zecchina. Random k-satisfiability problem: From an analytic solution to an efficient algorithm. *Physical Review E*, 66(5):056126, 2002.

[7] Marc Mézard, Giorgio Parisi, and Riccardo Zecchina. Analytic and algorithmic solution of random satisfiability problems. *Science*, 297:812–815, 2002.

[8] Alfredo Braunstein, Marc Mézard, and Riccardo Zecchina. Survey propagation: An algorithm for satisfiability. *Random Structures & Algorithms*, 27(2):201–226, 2005.

[9] Marc Mézard and Thierry Mora. Constraint satisfaction problems and neural networks: A statistical physics perspective. *Journal of Physiology-Paris*, 103(1):107–113, 2009.

[10] Daniel S. Fisher and David A. Huse. Equilibrium behavior of the spin-glass ordered phase. *Phys. Rev. B*, 38:386–411, Jul 1988.

- [11] Alexander K. Hartmann. Evidence for nontrivial ground-state structure of $3d \pm j$ spin glasses. *Europhys. Lett.*, 40, 1997.
- [12] A. Alan Middleton. Numerical investigation of the thermodynamic limit for ground states in models with quenched disorder. *Phys. Rev. Lett.*, 83:1672–1675, Aug 1999.
- [13] Giorgio Parisi. Some considerations of finite-dimensional spin glasses. *J. Phys. A: Math. Theor.*, 41, 2008.
- [14] Ryoichi Kikuchi. A theory of cooperative phenomena. *Physical review*, 81(6):988, 1951.
- [15] Guozhong An. A note on the cluster variation method. *Journal of Statistical Physics*, 52(3-4):727–734, 1988.
- [16] Alessandro Pelizzola. Cluster variation method in statistical physics and probabilistic graphical models. *Journal of Physics A: Mathematical and General*, 38(33):R309, 2005.
- [17] Jonathan S Yedidia, William T Freeman, and Yair Weiss. Bethe free energy, kikuchi approximations, and belief propagation algorithms. *Advances in neural information processing systems*, 13, 2001.
- [18] Jonathan S Yedidia, William T Freeman, Yair Weiss, et al. Generalized belief propagation. In *NIPS*, volume 13, pages 689–695, 2000.
- [19] Jonathan S Yedidia, William T Freeman, and Yair Weiss. Constructing free-energy approximations and generalized belief propagation algorithms. *Information Theory, IEEE Transactions on*, 51(7):2282–2312, 2005.
- [20] Tommaso Rizzo, Alejandro Lage-Castellanos, Roberto Mulet, and Federico Ricci-Tersenghi. Replica cluster variational method. *Journal of Statistical Physics*, 139(3):375–416, 2010.
- [21] A. Lage-Castellanos, R. Mulet, F. Ricci-Tersenghi, and T. Rizzo. Replica cluster variational method: the replica symmetric solution for the 2d random bond ising model. *J. Phys. A: Math. Theor.*, 46, 2013.
- [22] A Lage-Castellanos, R Mulet, and F Ricci-Tersenghi. Message passing and monte carlo algorithms: Connecting fixed points with metastable states. *EPL (Europhysics Letters)*, 107(5):57011, 2014.
- [23] Gino Del Ferraro, Hai-Jun Zhou, and Erik Aurell. A new approach to gsp, 2015. In preparation.
- [24] Haijun Zhou, Chuang Wang, Jing-Qing Xiao, and Zedong Bi. Partition function expansion on region graphs and message-passing equations. *Journal of Statistical Mechanics: Theory and Experiment*, 2011(12):L12001, 2011.
- [25] Haijun Zhou and Chuang Wang. Region graph partition function expansion and approximate free energy landscapes: Theory and some numerical results. *Journal of Statistical Physics*, 148(3):513–547, 2012.
- [26] Chuang Wang and Hai-Jun Zhou. Simplifying generalized belief propagation on redundant region graphs. *arXiv preprint arXiv:1304.5112*, 2013.
- [27] Samuel Frederick Edwards and Phil W Anderson. Theory of spin glasses. *Journal of Physics F: Metal Physics*, 5(5):965, 1975.
- [28] Ingo Morgenstern and K Binder. Magnetic correlations in two-dimensional spin-glasses. *Physical Review*

B, 22(1):288, 1980.

- [29] Lawrence Saul and Mehran Kardar. Exact integer algorithm for the two-dimensional $\pm j$ ising spin glass. *Physical Review E*, 48(5):R3221, 1993.
- [30] T Jörg, J Lukic, E Marinari, and OC Martin. Strong universality and algebraic scaling in two-dimensional ising spin glasses. *Physical review letters*, 96(23):237205, 2006.
- [31] Creighton K Thomas, David A Huse, and A Alan Middleton. Zero-and low-temperature behavior of the two-dimensional $\pm j$ ising spin glass. *Physical review letters*, 107(4):047203, 2011.
- [32] Creighton K Thomas and A Alan Middleton. Exact algorithm for sampling the two-dimensional ising spin glass. *Physical Review E*, 80(4):046708, 2009.